Thin Solid Films 517 (2009) 6809–6816

Contents lists available at ScienceDirect

Thin Solid Films

journal homepage: www.elsevier.com/locate/tsf

The surface chemistry of 3-mercaptopropyltrimethoxysilane films deposited on magnesium alloy AZ91

A. Scott, J.E. Gray-Munro *

Dept. of Chemistry and Biochemistry, Laurentian University, Sudbury, Ontario, Canada P3E 2C6

ARTICLE INFO

Article history:
Received 1 October 2007
Received in revised form 22 May 2009
Accepted 26 May 2009
Available online 2 June 2009

Keywords:
Magnesium alloy
Organosilane
X-ray photoelectron spectroscopy
ATR-FTIR
Infrared

ABSTRACT

Magnesium and its alloys have desirable physical and mechanical properties for a number of applications. Unfortunately, these materials are highly susceptible to corrosion, particularly in the presence of aqueous solutions. The purpose of this study is to develop a uniform, non-toxic surface treatment to enhance the corrosion resistance of magnesium alloys. This paper reports the influence of the coating bath parameters and alloy microstructure on the deposition of 3-mercaptopropyltrimethoxysilane (MPTS) coatings on magnesium alloy AZ91. The surface chemistry at the magnesium/MPTS interface has also been explored. The results indicate that the deposition of MPTS onto AZ91 was influenced by both the pH and MPTS concentration in the coating bath. Furthermore, scanning electron microscopy results showed that the MPTS film deposited uniformly on all phases of the magnesium alloy surface. X-ray photoelectron spectroscopy studies revealed that at the magnesium/MPTS interface, the molecules bond to the surface through the thiol group in an acid–base interaction with the $Mg(OH)_2$ layer, whereas in the bulk of the film, the molecules are randomly oriented.

1. Introduction

Magnesium and its alloys have excellent mechanical properties with a specific density that is 1/4 that of steel and 2/3 that of aluminum. These properties make it a desirable light weight construction material for a number of applications. Unfortunately, these materials are also highly susceptible to corrosion, particularly in the presence of aqueous solutions [1]. This has limited their use in the automotive, aerospace and biomedical industries, where exposure to solutions containing ions such as chloride, sulphate and phosphate is unavoidable. In order to improve the corrosion resistance of magnesium and its alloys, protective coatings can be applied [1]. However, the development of protective coatings on high aluminum content magnesium alloys has proven to be a challenge for these materials [1]. This is due to both their multi-phase surface microchemistry and rapid surface oxidation. In particular, the formation of intermetallic ($Mg_{17}Al_{12}$) species at the grain boundaries, results in a non-uniform surface which greatly complicates the coating process [1].

Organosilanes are ambifunctional molecules with the general structure $(R'O)_3Si–R–X$ [2]. Where R is an alkyl chain, R′ is typically CH_3 or C_2H_5 and X can be a number of different functional groups such as S–H, $–NH_2$, –OH and –COOH. The X group is typically chosen for its ability to interact with a specific organic coating or molecule that will be subsequently deposited on top of the organosilane layer.

These molecules are commonly used as adhesion promoters between inorganic substrates and organic coatings.

The alkoxysilane part of the molecule can covalently bond with a variety of mineral or metal surfaces through complex hydrolysis/condensation reactions where Si–O–Metal bonds are ultimately formed. These reactions are typically done by immersing the substrate in an organic solvent that may also contain small amounts of water.

In order to bond to the surface, organosilanes must undergo both hydrolysis and condensation reactions. These reactions are shown below:

$$RSi(OR')_3 + 3H_2O \rightarrow RSi(OH)_3 + 3R'OH—\text{Hydrolysis} \quad (1)$$

$$RSi(OH)_3 + MOH \rightarrow RSi(OH)_2–O–M + H_2O—\text{Condensation.} \quad (2)$$

It is commonly believed that organosilanes can only undergo condensation reactions with a metal surface after hydrolysis of the molecule in solution has occurred. However, some researchers have speculated that the silanes may initially hydrogen-bond with the substrate and then subsequently form covalent bonds upon curing [3]. The rate of hydrolysis depends on several factors, such as the functional group (X) on the alkyl chain, the availability of water and the pH of the coating bath [4,5]. In general, the rate of hydrolysis has been shown to increase at lower pH while the condensation reaction is favoured at higher pH [4]. The condensation reaction can occur either between the organosilane molecules themselves or with the substrate surface. The net reaction, a sum of the hydrolysis and

* Corresponding author.
E-mail address: jgray@laurentian.ca (J.E. Gray-Munro).

0040-6090/$ – see front matter
doi:10.1016/j.tsf.2009.05.044

condensation steps, is dependent on the availability of water, the nature of the surface to be grafted, the chemical functionality of the silane and the pH of the original solution [5]. The quality of the coating produced is also affected by factors such as curing and solution concentration. For example, it has been found that curing of the film after deposition leads to better cross-linking between the organosilane molecules. Furthermore; the solution concentration has been shown to have a significant influence on the film thickness [3].

Although organosilanes are most commonly used as adhesion promoters, these coatings have also been shown to improve formability [7], enhance corrosion resistance [8,9], increase scratch resistance [7] and improve wear resistance [10] of a variety of different materials. They have become of considerable interest for treating aluminum alloys because they have been shown to provide both corrosion protection and improved adhesion [6].

Although the interaction of these molecules with materials such as silicon, aluminum and steel has been studied, relatively little has been reported on their interaction with magnesium alloy surfaces [11–13]. Both Zucchi et al. and Khramov et al. reported that organosilane based coatings positively impact the corrosion resistance of magnesium alloys. Zucchi et al. further proposed that the Si–O–Mg interaction should be strong due to the strong affinity of the silanol (–Si–O–H) functional group for basic oxides. However, Mitchell et al. reported that the chemical structure of the organosilane played a significant role in the stability of the coatings produced and that coating thickness plays a critical role in the protective properties of the organosilane film.

The purpose of this study was to investigate:

1. The influence of pH, solution concentration and deposition time on organosilane film formation on AZ91 magnesium alloy substrates.
2. The influence of the substrate surface microchemistry on the coating uniformity.
3. The nature of the chemical interaction at the organosilane/magnesium substrate interface.

The organosilane of interest in this study was 3-mercaptopropyltrimethoxysilane (MPTS). This organosilane is of particular interest due to the strong interaction of thiols with silver [14]. This could be of benefit for the use of organosilanes as a pre-treatment prior to electroless plating on magnesium alloys. The chemical structure of the organosilane used in this study is shown in Fig. 1.

2. Experimental details

2.1. Sample preparation

Prior to coating, Mg alloy AZ91 plates (Lunt Technologies Inc.) were cut into 1 inch by 1/2 inch coupons and were sequentially polished to a 1 micron surface finish with diamond suspension polishing oil purchased from Buehler. After polishing, the samples were ultrasonically degreased in acetone followed by methanol and finally deionized water in order to remove any excess oil. In order to remove residual organics and to increase the concentration of hydroxyl groups at the magnesium alloy surface, the samples were immersed in a 0.5 M NaOH (pH 12) solution at 50 °C for 1 h. An increase in surface hydroxyl groups should increase the basicity of the substrate and thus improve the level of condensation with the sample surface [11]. Finally the polished, degreased, alkaline aged samples were rinsed with deionized water.

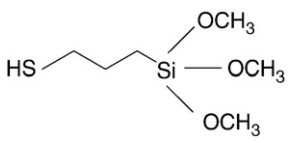

Fig. 1. Molecular structure of 3-mercaptopropyltrimethoxysilane.

All solvents and chemicals were purchased from Sigma Aldrich and were used without further purification.

2.2. 3-Mercaptopropyltrimethoxysilane coating

All coating baths were prepared with a 2:3% ratio (v/v) of MPTS to water, in methanol as a solvent. For example 100 ml of a 2% silane solution would contain 2 ml of silane, 3 ml of water and 95 ml of methanol. The pH of the bath was adjusted with either dilute sulphuric acid or dilute sodium hydroxide as required. Unless otherwise stated, the MPTS solutions were stirred at ambient temperature for 24 h in order to ensure complete hydrolysis of the Si–O–R bonds to Si–O–H. The Mg alloy coupons were dip coated in the MPTS solution for varying deposition times. Upon removal, the coupons were air dried and cured at 100 °C for 1 h. The organosilanes were purchased from Sigma Aldrich and were used without further purification.

2.3. Surface characterization

The magnesium alloy surfaces were characterized by a combination of attenuated total reflection-Fourier transform infrared spectroscopy (ATR-FTIR), X-ray photoelectron spectroscopy (XPS), scanning electron microscopy (SEM) and Energy Dispersive Spectroscopy (EDS).

ATR-FTIR spectra were collected using a Bruker Optics IR microscope with an ATR objective and a liquid nitrogen cooled mercury cadmium telluride detector. Each spectrum is the result of 1000 scans at a resolution of 4 cm^{-1}. The spectra were then corrected for atmospheric CO_2 and H_2O with the atmospheric compensation function that was available with the software.

SEM images coupled with EDS spectra were obtained using a JEOL scanning electron microscope. The electron beam current was 1.0 nA. The vacuum in the analysis chamber was 1.5×10^{-4} Pa and the working distance of the microscope was 8.5–9.0 mm. EDS spectra were collected over 45 second intervals.

XPS spectra were recorded with a Kratos Axis Ultra X-Ray photoelectron spectrometer. The XPS was performed in a vacuum at 1.3×10^{-7} Pa with a take off angle of 90°, except for the angle resolved XPS spectra where the take off angle was varied from 90° to 15°. The survey scans were recorded over a spot size of 1000 μm between 0 and 1000 eV. Sample analysis was performed in triplicate. The reported data is averaged over 3 samples with the standard deviation reported as the error. The surface atomic % of each species was calculated after identification of each element according to its binding energy, using the appropriate Schofield factors provided by the Kratos software. The high resolution spectra were recorded over an area of 300×700 μm with a pass energy of 20 eV. All high resolution spectra were charge corrected to the C–C bond in the C (1s) spectrum at 285.0 eV.

3. Results and discussion

3.1. Influence of coating bath pH

The influence of coating bath pH was investigated for pH 4, 7 and 10 solutions. The surface chemistry and morphology of the films deposited from each solution were studied by a combination of ATR-FTIR and SEM/EDS. Fig. 2 shows the ATR-FTIR spectra obtained for organosilane coatings deposited from pH 4, 7 and 10 solutions. Characteristic peaks for MPTS were observed on the magnesium alloy coupons at all 3 pH values. The low intensity peak at 2543 cm^{-1} is characteristic of the S–H stretching band for the thiol group [15]. The absorption peaks at 1249 cm^{-1} and 1108 cm^{-1} are due to Si–C stretching and Si–O stretching respectively [15]. The broad absorption band at around 1500 cm^{-1} is due to the presence of carbonate at the surface of the substrate. Magnesium alloys react with atmospheric carbon dioxide to form surface magnesium carbonate.

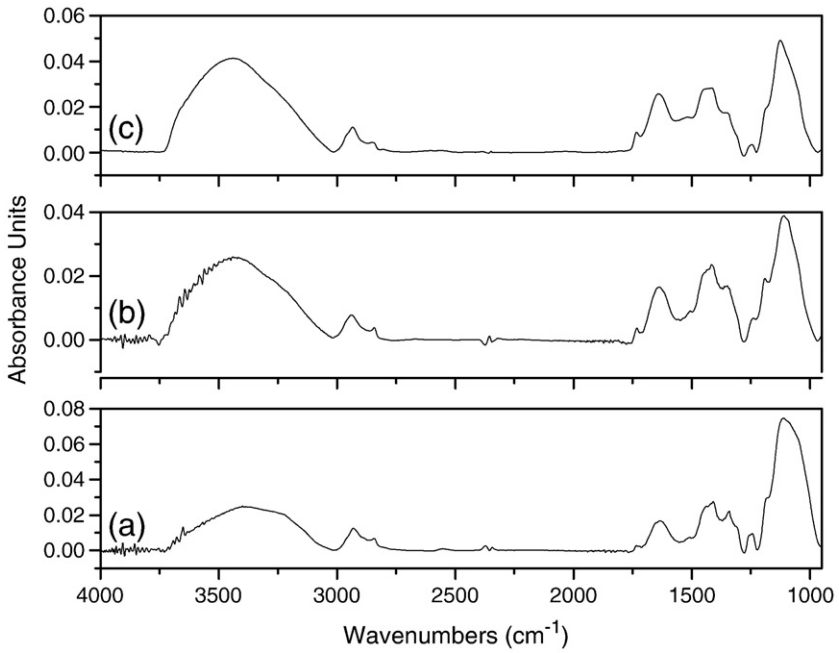

Fig. 2. ATR-FTIR spectra for MPTS coatings (4%) on magnesium alloy AZ91 as a function of pH; (a) pH 4, (b) pH 7 and (c) pH 10.

Fig. 3 shows SEM images for the coated magnesium alloy coupons at the three different pH values. In all three images the microstructure of the magnesium alloy can be clearly observed. The darker regions in the images are the magnesium rich primary α phase. The lighter regions are the β phase, these are aluminum rich regions consisting of $Mg_{17}Al_{12}$. Along the grain boundaries, between the primary α phase and the β phase is the eutectic α phase [16]. This region is also aluminum rich but the concentration of aluminum gradually decreases from the center of the β phase grain until the α phase is reached [16]. Fig. 3a is an SEM image of the MPTS film deposited from a pH 4 solution. The SEM analysis shows complete coverage of the substrate by MPTS at pH 4, indicating uniform deposition of the organosilane at pH 4.

Fig. 3b shows an SEM image of the MPTS film deposited at pH 7. Pitting was observed on these sample surfaces and chemical analysis by EDS did not detect appreciable amounts of Si or S at the surface. This indicates that although some MPTS is detected by infrared analysis the amount of MPTS adsorbed at pH 7 is very low.

Fig. 3c shows an SEM image of the MPTS film deposited at pH 10. At the higher pH value, obvious condensation of MPTS oligomers was observed in solution prior to coating. These oligomers were subsequently adsorbed to the magnesium alloy surface upon immersion of the coupon in the bath. It is obvious from the SEM image that the MPTS deposition is non-uniform. Chemical analysis of the sample by EDS revealed that only the dark area in the SEM images contained sulphur and silicon while no sulphur or silicon was detected on the rest of the surface.

The SEM/EDS results clearly indicate that the highest levels of adsorption and most uniform films are obtained when the coating bath is at a pH of 4. It is clear that at pH 10 the rate of intermolecular condensation between the organosilane molecules themselves exceeds the rate of condensation between the organosilane and the metal surface. In fact it has been previously reported that high concentrations of oligomers in solution leads to non-uniform organosilane films [5]. At a pH of 7 very little deposition was observed. This is likely due to incomplete hydrolysis of the organosilane molecules which leads to little condensation with the surface. It has been previously reported that the presence of unhydrolyzed groups can also result in a non-uniform surface film [3].

At a pH of 4, the most uniform films were obtained, this pH was thus chosen as the optimum pH for our coating bath.

3.2. Influence of substrate microstructure

More detailed chemical analysis of the surface of the organosilane deposited at pH 4 was performed to determine the influence of the substrate microstructure on the uniformity of the organosilane films. EDS analysis of the magnesium rich α phase of the material and the aluminum rich β phase of the material reveals the presence of equal amounts of silicon and sulphur on each phase of the alloy. The atomic percentages are given in Table 1. This indicates that the organosilane adsorbs equally on both phases of the alloy regardless of differences in microchemistry across the surface of the material.

3.3. Influence of pre-treatment by alkaline ageing

Alkaline ageing was performed by immersing the samples in a pH 12 sodium hydroxide solution prior to coating with MPTS. The objective of this pre-treatment was to increase the surface concentration of the hydroxyl groups on the magnesium alloy surface and thus increase the rate of the condensation reaction between the magnesium alloy surface and the organosilane. At high pH values, the Pourbaix diagram for magnesium indicates that magnesium hydroxide is the thermodynamically stable phase. The surface chemistry of the magnesium alloy coupons before and after alkaline ageing was compared to determine the influence of this pre-treatment on the surface chemistry of the magnesium alloy.

ATR-FTIR spectra of polished and alkaline aged samples are shown in Fig. 4. Both of these two spectra have a broad peak at about 1500 cm^{-1} due to the presence of carbonate at the alloy surface. It is well known that magnesium is an extremely reactive metal and metallic magnesium is not present at its surface. Rather, it undergoes reactions with oxygen, water vapour and carbon dioxide in the atmosphere to form magnesium oxide/hydroxide and magnesium carbonate surface layers. Both spectra also show a sharp absorption band at about 3600 cm^{-1}. After alkaline ageing, there was a large increase in the surface concentration of Mg $(OH)_2$, as evidenced by the increase in intensity of the characteristic

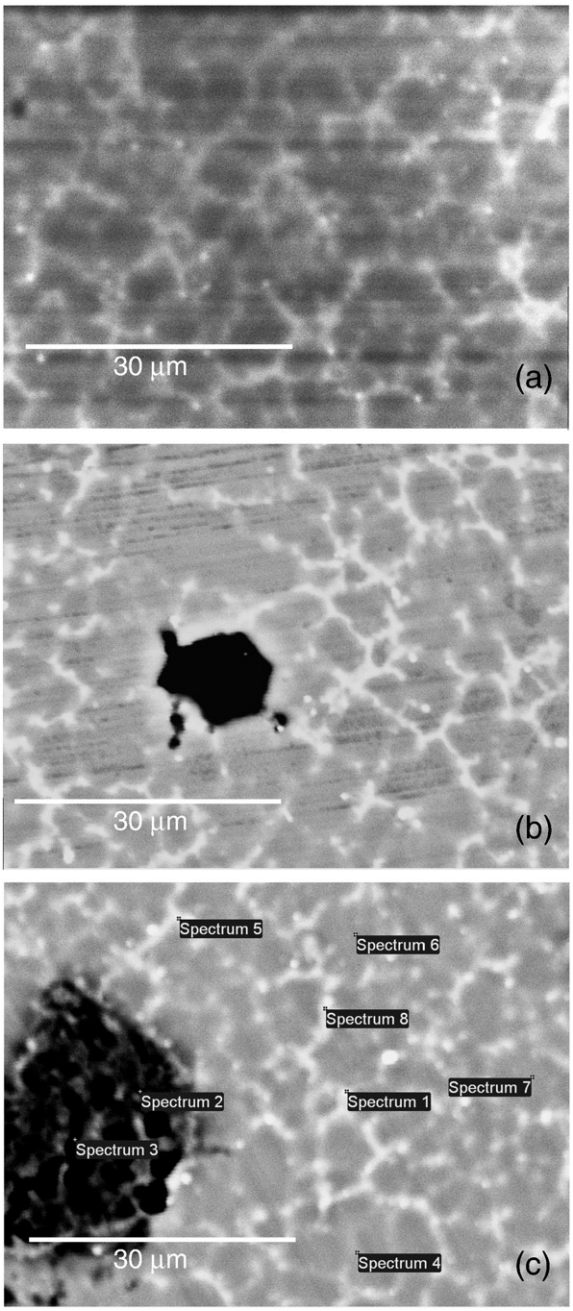

Fig. 3. SEM images of MPTS coatings (4%) on magnesium alloy AZ91 as a function of pH; (a) pH 4, (b) pH 7 and (c) pH 10.

absorption band of this compound at 3600 cm^{-1} [17]. A concomitant decrease in the intensity of the carbonate absorption was also observed.

X-ray photoelectron spectroscopy was used to investigate changes in the chemistry of the first 5–10 nm of the sample surface as a result of pre-treatment by alkaline ageing. High resolution spectra of the Mg 2p peak for polished and alkaline aged samples are compared in Fig. 5. Prior to alkaline ageing the magnesium 2p spectrum can be deconvoluted into 2 peaks, one at 49.87 eV and one at 50.95 eV. These two peaks can be attributed to magnesium hydroxide and magnesium carbonate respectively [18]. Magnesium is known to rapidly oxidize in the atmosphere and in the presence of aqueous solutions. Due to our processing conditions, it is therefore highly unlikely that any metallic magnesium remains at the surface, in fact we know that even prior to alkaline ageing there is a significant amount of magnesium hydroxide detected by FTIR on the sample surface. The presence of carbonate was also observed by FTIR, therefore, the two techniques coupled together indicate the presence of magnesium hydroxide and magnesium carbonate at the sample surface prior to alkaline ageing. It is likely that some magnesium oxide is also present at this stage. After alkaline ageing there is a significant increase in the intensity of the peak at 49.8 eV (from 45% prior to alkaline ageing to 80% after the pre-treatment). The FTIR spectra also show an increase in magnesium hydroxide at the surface which confirms that the growth in this peak must be due to an increase in surface hydroxyl concentration. Furthermore the decrease in the higher binding energy peak correlates with the observed decrease in carbonate on the alloy that was observed by FTIR. Taken together, the XPS and FTIR results suggest that alkaline ageing of the samples results in an increase in magnesium hydroxide at the sample surface coupled with a decrease in magnesium carbonate.

High resolution spectra of the Al 2p peak for polished and alkaline aged samples are compared in Fig. 5. Prior to alkaline ageing, the Al 2p peak can be deconvoluted into 2 peaks at 72.7 eV and 74.86 eV. These binding energies correspond to metallic aluminum (22% of peak envelope) [19] and aluminum hydroxide (78% of peak envelope) [20] respectively. This indicates that both metallic aluminum and aluminum hydroxide were present at the surface prior to alkaline ageing, likely due to the slower oxidation rate of this metal. After alkaline ageing only one peak is observed at a binding energy of 74.6 eV. The loss of the peak at 72.7 eV indicates that alkaline ageing results in complete conversion of the aluminum at the surface to aluminum hydroxide.

The corresponding high resolution XPS spectra of the O 1s peak for polished and alkaline aged samples are compared in Fig. 5. Both of these spectra can be deconvoluted into two peaks corresponding to magnesium hydroxide (lower binding energy peak) and carbonate species (higher binding energy peak) [18]. After alkaline ageing the peak due to magnesium hydroxide grows while the peak due to magnesium carbonate decreases in intensity. This corresponds with the observed changes in the carbonate peak of the C 1s spectra for these samples (Fig. 5). The highest binding energy peak in the C 1s spectrum can be attributed to carbonate. There is a 50% decrease in this peak after alkaline ageing. These results further support our assertion that alkaline ageing increases the concentration of the hydroxyl groups at the alloy surface and removes organic contaminants.

Overall, the XPS results for Mg 2p, Al 2p and O 1s all show an increase in the surface concentration of hydroxyl groups after alkaline ageing. A decrease in the carbonate peaks for the Mg 2p, O 1s and C 1s spectra is also observed. These XPS results compliment the increase in surface hydroxyl and decrease in surface carbonate that were observed on alkaline aged samples by ATR-FTIR. These results indicate that the overall influence of alkaline ageing was to increase the surface concentration of hydroxyl groups on the magnesium alloy surface. This should result in an increase in the rate of the condensation reaction between the magnesium alloy surface and the organosilane.

3.4. Influence of MPTS concentration in the coating bath

The influence of coating bath concentration on the deposition of MPTS films onto alkaline aged magnesium alloy samples was studied as a function of solution concentration by both ATR-FTIR and XPS. The concentration of MPTS in the coating bath ranged from a low concentration of 0.1% to a high concentration of 4% MPTS. The

Table 1
EDS analysis of atomic % silicon and sulphur on α phase and β phase of magnesium alloy AZ91.

	Atomic % silicon	Atomic % sulphur
α phase of AZ91	9.51% ± 1.35	6.73% ± 1.18
β phase of AZ91	8.83% ± 1.33	6.11% ± 1.18

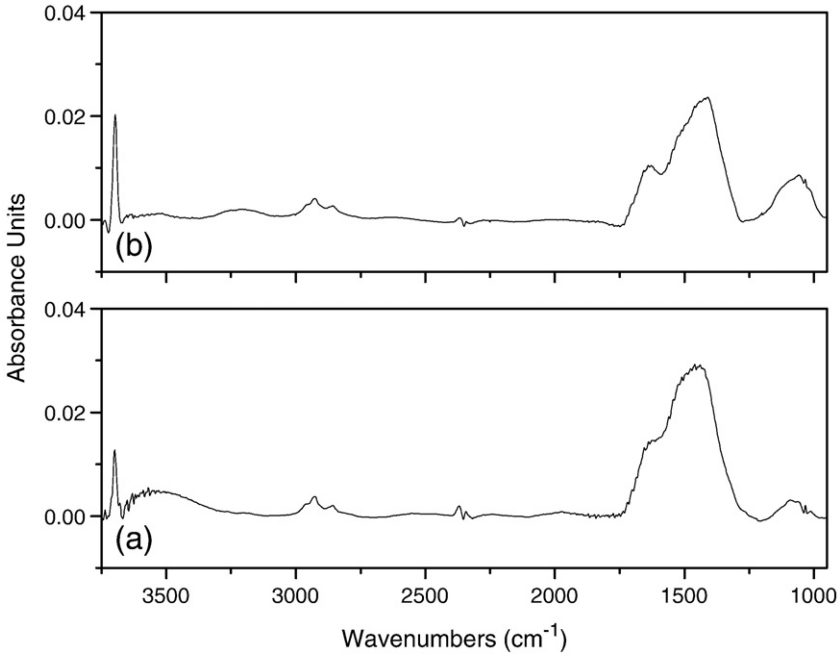

Fig. 4. ATR-FTIR spectra of (a) polished magnesium alloy and (b) alkaline aged magnesium alloy.

deposition time was fixed at 2 min. Fig. 6a shows the ATR-FTIR spectra of the MPTS films as a function of increasing concentration. Increases in the intensities of the S–H stretching band for the thiol group at 2543 cm^{-1}, the Si–C stretch at 1249 cm^{-1} and the Si–O stretch at 1108 cm^{-1} were observed [15]. These bands are all characteristic absorption bands for MPTS. A decrease in the intensity of the two peaks that are due to the substrate (carbonate at 1500 cm^{-1} and magnesium hydroxide at 3600 cm^{-1}) is also observed as the organosilane film

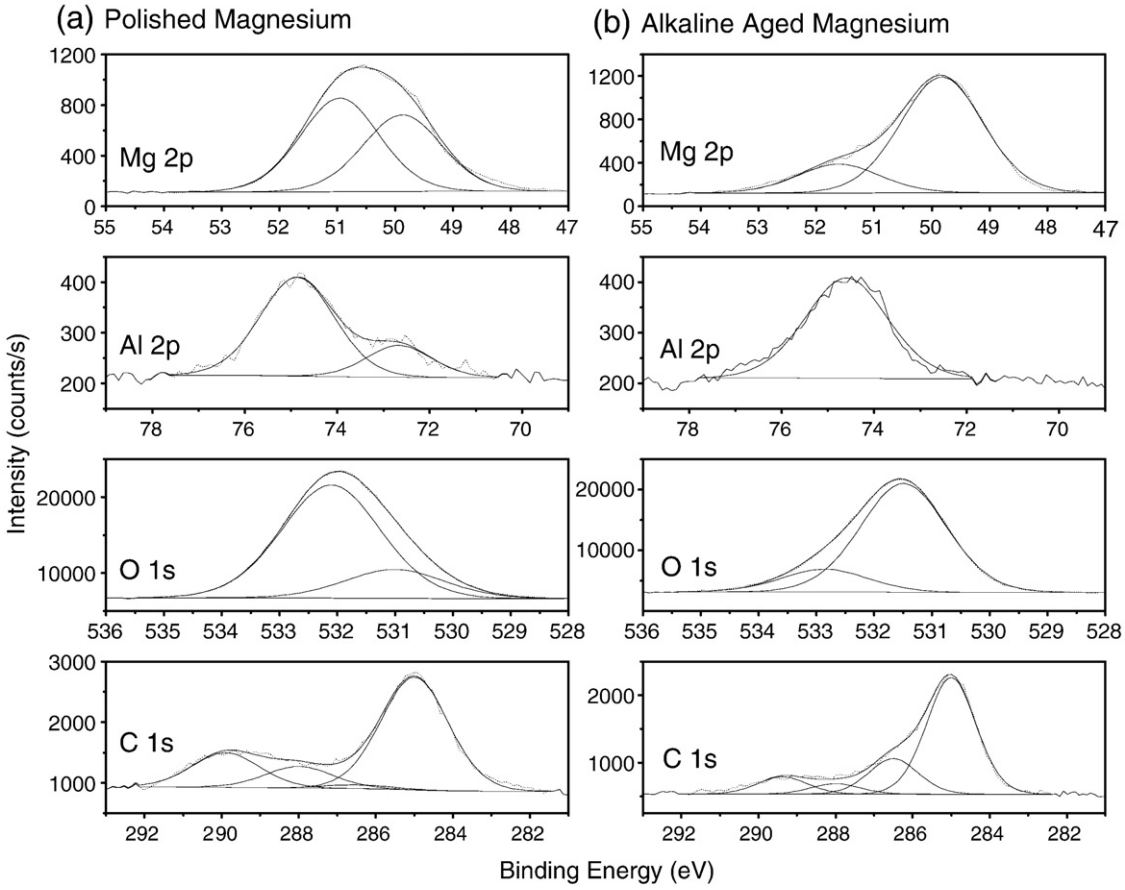

Fig. 5. High resolution XPS of the Mg 2p, Al 2p, O 1s and C 1s spectral regions for (a) polished magnesium alloy and (b) alkaline aged magnesium alloy.

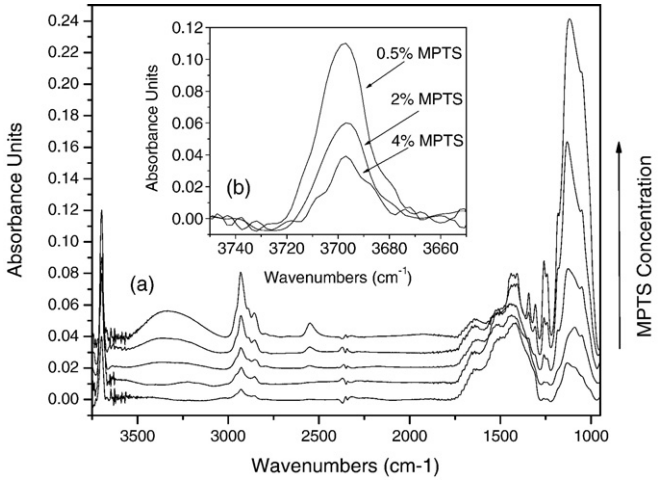

Fig. 6. ATR-FTIR spectra for MPTS coatings on magnesium alloy substrates as a function of MPTS concentration in the coating bath; (a) full spectrum, and (b) expanded OH stretch region.

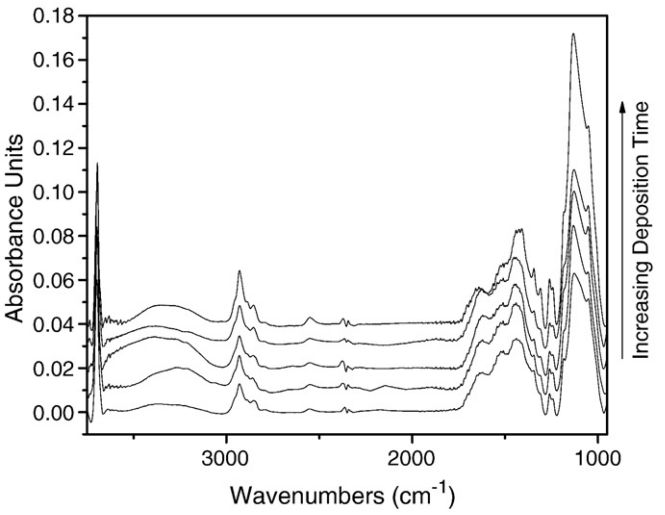

Fig. 8. ATR-FTIR spectra for MPTS coatings on magnesium alloy substrates as a function of immersion time in the coating bath.

thickness increases. Fig. 6b shows the OH stretch region of the spectrum in more detail. It is very clear that this peak decreases with increasing silane film thickness.

The influence of silane concentration on film thickness was also evaluated by XPS. Fig. 7 is a graph of atomic % Si and atomic % Mg detected by XPS as a function of solution concentration. This graph shows that there is a linear increase in atomic % Si with increasing solution concentration up to 1% after which the curve plateaus. The plateau indicates that the thickness of the film has exceeded the sampling depth of the XPS. There is a corresponding decrease in % Mg with increasing solution concentration up to 1% after which the measured surface concentration of magnesium drops to zero. This increase in atomic % of silicon coupled with a decrease in the observed surface concentration of magnesium indicates that the thickness of the films increases as the solution concentration of silane in the coating bath increases.

3.5. Influence of deposition time

The influence of deposition time on the amount of MPTS deposited onto alkaline aged magnesium alloy samples was also studied by immersing the samples into the coating bath for various immersion times by both ATR-FTIR and XPS. The solution concentration of MPTS was fixed at 1% and the deposition times ranged from 2 min to 30 min.

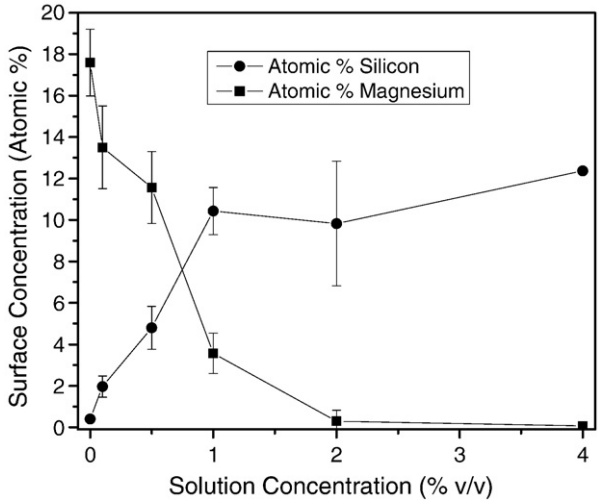

Fig. 7. Graph of XPS atomic % of silicon and magnesium as a function of MPTS concentration in the coating bath.

Fig. 8 shows ATR-FTIR spectra of the MPTS films obtained as a function of deposition time. Upon comparison of the intensities of several of the characteristic absorption bands of MPTS (see Section 3.4) it was observed that there was very little difference in signal intensity for samples immersed in the silane coating bath from 2 min to 15 min. There is a modest increase in the intensity of the IR bands after immersion in the bath for 30 min. The influence of deposition time was also studied by XPS for a 0.5% MPTS solution with deposition times of 2, 5 and 15 min with XPS. A low concentration was chosen to ensure that we would not exceed the sampling depth of XPS and consequently be able to determine film growth. The XPS survey scans showed the presence of magnesium at the surface for all of these samples indicating that the film thickness was less than 5–10 nm. Fig. 9 is a plot of the Si/Mg ratio as a function of deposition time. It is immediately obvious from this plot that there was no significant change in film thickness as a function of deposition time.

3.6. Surface chemistry at the magnesium/MPTS interface

High resolution spectra for the S 2p peak of the organosilane as a function of increasing film thickness are shown in Fig. 10. Fig. 10a is the high resolution sulphur spectrum for a very thin film, deposited from a 0.1% MPTS for 2 min. This spectrum has been deconvoluted into 4 peaks. The high resolution spectrum for sulphur is a doublet

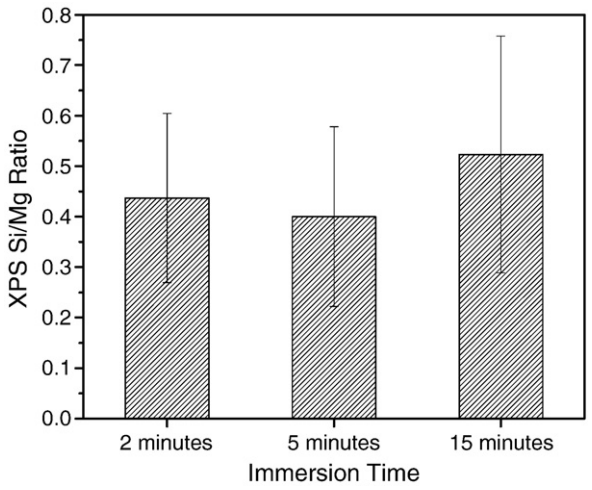

Fig. 9. Graph of XPS Si/Mg ratio as a function of immersion time in the coating bath.

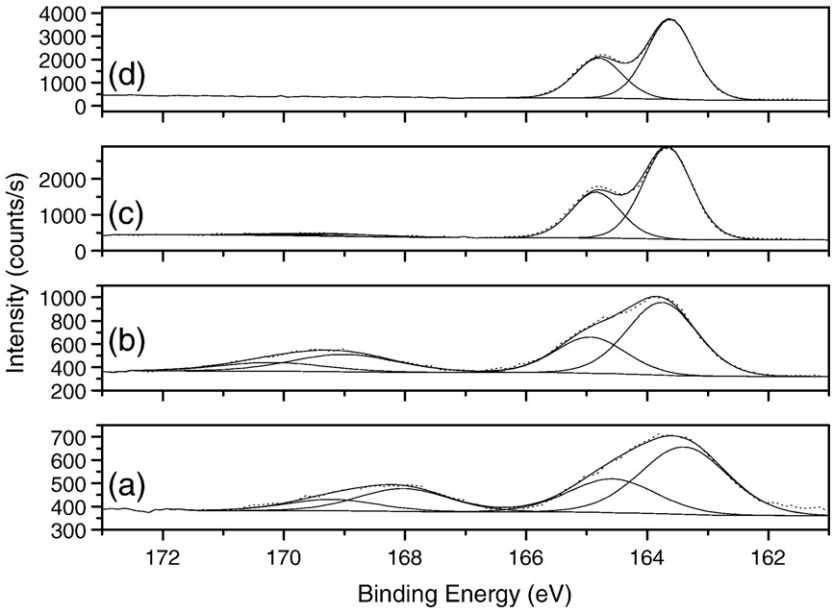

Fig. 10. High resolution S 2p XPS spectra of (a) 0.1% MPTS coating bath, (b) 2% MPTS coating bath and (c) 4% MPTS coating bath.

consisting of separate peaks for the $2p_{1/2}$ and $2p_{3/2}$ photoelectrons. The fact that the sulphur spectrum for this sample has 4 peaks indicates that sulphur is present in two different chemical environments. There is both sulphate and thiol present on the surface of the MPTS coated Mg alloy AZ91. The binding energy for the sulphate is at 169.21 eV and 168.03 eV, and the lower binding energy at 164.58 eV and 163.40 eV is for the thiol [21]. As the solution concentration increases our previous infrared results indicated that the film thickness also increases which means that the amount of thiol at the surface must increase. This is confirmed in the S 2p XPS spectra for the 2% and 4% MPTS films. As the solution concentration increases the S 2p peak due to thiol increases and the S 2p peak due to sulphate gradually disappears. The disappearance of the sulphate peak as the silane film thickness increases indicates that the sulphate is present at the Mg/MPTS interface and not the MPTS/air interface. This suggests that the sulphate peak is not due to oxidation of the organosilane thiol groups but that there must be some other source of sulphate at the Mg/MPTS interface.

In order to identify the source of the sulphate at the Mg/MPTS interface, a magnesium alloy sample was exposed to a mock coating bath for 2 min. This mock coating bath contained all of the coating bath components except MPTS. The infrared spectrum for the sample exposed to the mock coating bath is shown in Fig. 11. Upon comparison with the infrared spectrum of an alkaline aged Mg alloy sample a new absorption band is observed. There is a large broad peak at 1129 cm^{-1} with a small shoulder at 1056 cm^{-1}. This peak can be attributed to the presence of sulphate at the surface of the magnesium alloy sample [22]. The source of this sulphate is due to the sulphuric acid that is used to lower the pH of the coating bath and not due to oxidation of the MPTS thiol groups. This peak was not observed by ATR-FTIR in the presence of a silane film because the sulphate absorption overlaps with the Si–O absorption from the MPTS. The formation of magnesium sulphate in the coating bath explains why sulphate is only observed at the Mg/MPTS interface. This result is interesting because it indicates that there may be competing reactions occurring in the coating bath, the condensation of MPTS onto the Mg alloy AZ91 surface and the formation of $MgSO_4$.

Examination of the changes in the binding energies of the substrate peaks after coating with MPTS reveals that there is an increase in the binding energy of the Al 2p peak previously attributed to Al $(OH)_3$ from 74.6 eV to 75.4 eV. An increase in the binding energy of the $Mg(OH)_2$ peak from 49.87 eV to 50.3 eV is also observed after coating with MPTS. This indicates that there is a strong interaction between the metal hydroxides and the MPTS molecules.

The binding energy of the S 2p1/2 peak for the 4% organosilane film is at a binding energy of 164.8 eV. The thickness of this film exceeds the sampling depth of the instrument therefore this binding energy should be representative of organosilane molecules that are not interacting with the substrate surface. The binding energy of the S 2p1/2 peak for the 0.1% organosilane film is at a slightly lower binding energy of 164.6 eV. The organosilane molecules in this film are interacting with the substrate. This decrease in binding energy suggests that the thiol group may be interacting directly with the substrate. Although organosilanes are commonly believed to interact with metal surfaces through a Si–O–Metal bond, it has been previously postulated that these molecules can interact with the surface in acid–base interactions depending on the nature of the functional group attached to the alkyl chain [21]. The two possible

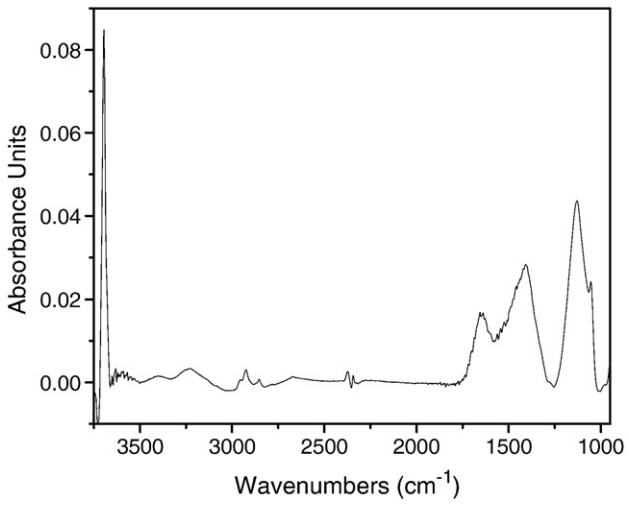

Fig. 11. ATR-FTIR spectrum of Mg alloy AZ91 exposed to a mock MPTS bath for 2 min.

orientations of the MPTS molecules are shown in Fig. 12 [21]. In Fig. 12a, the MPTS molecule is interacting with the surface hydroxide through an Si–O–Metal bond. In the second image, the MPTS molecule is interacting with the surface through the thiol group via hydrogen bonding.

In order to confirm the orientation of the MPTS molecules on the magnesium alloy surface, XPS spectra as a function of take off angle were collected. As the take off angle decreases, the sampling depth of the instrument also decreases. This means that if the thiol groups are pointing away from the surface, an increase in S/Si ratio should be observed as the take off angle decreases [21]. The results from this experiment are summarized in Fig. 13. Our previous XPS results indicated that an MPTS film prepared from a 0.1% solution is thin enough to allow sampling of the magnesium/MPTS interface. For these thin MPTS layers a decrease in S/Si ratio from approximately 1 to 0.7 is observed as the take off angle is decreased. This confirms that the MPTS molecules at the magnesium/MPTS interface are interacting with the substrate through an acid–base interaction between the magnesium hydroxide layer and the thiol functional group [21]. In contrast, MPTS films prepared from a 2% solution are thick enough that the silane film itself exceeds the sampling depth of the instrument. In these thicker films where the interface is not probed, the S/Si ratio remains approximately 1 at all take off angles. This indicates that the MPTS molecules in subsequent layers of the silane film are randomly oriented [21].

4. Conclusions

The influence of coating bath parameters, substrate microstructure and pre-treatment on the deposition of MPTS onto magnesium alloys has been discussed. The surface chemistry of the magnesium/MPTS interface has also been studied. These studies have shown that MPTS coatings are uniformly deposited on all phases of the AZ91 magnesium alloy surface at a pH of 4. The concentration of the MPTS coating bath was found to have a significant influence on film thickness while deposition time was shown to have little effect on the overall film thickness. Furthermore, these studies reveal that the oxide layer of Mg alloy AZ91 can be altered through alkaline ageing and that the increase in surface hydroxide concentration results in a strong interaction between the MPTS molecules and the magnesium alloy substrate. At the magnesium/MPTS interface, this interaction is an acid–base interaction between the thiol group of the MPTS molecule and the basic magnesium hydroxide substrate. Conversely, the MPTS molecules in subsequent layers of the coating are randomly oriented.

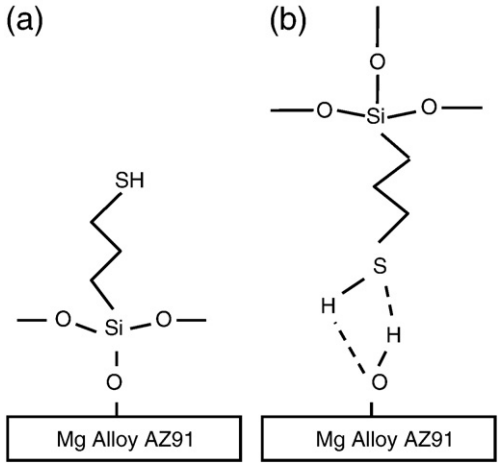

Fig. 12. Schematic diagram of possible orientations for an MPTS molecule at the magnesium/MPTS interface (a) bonding through an Mg–O–Si bond and (b) bonding through an acid–base interaction between Mg–OH and S–H.

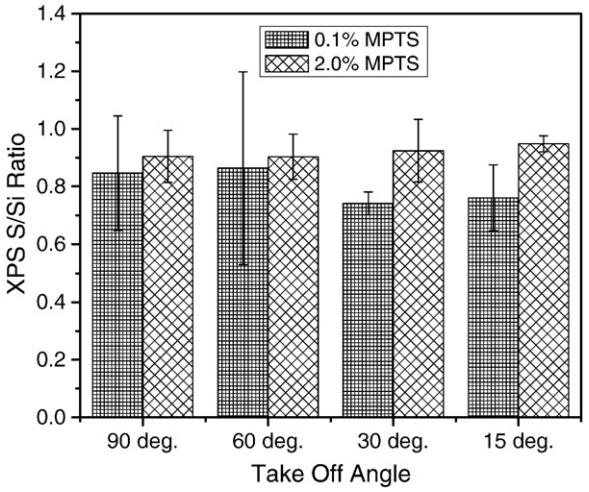

Fig. 13. Graph of S:Si ratio of 0.1% and 2% MPTS as a function of XPS take off angle (deposition time = 2 min).

Acknowledgements

The authors gratefully acknowledge the financial support of the Ontario Centers of Excellence, Meridian Technologies Inc., the Canada Foundation for Innovation and the Ontario Research Fund. We would also like to thank Mr. Mark Biesinger of Surface Science Western for his help with the X-ray photoelectron spectroscopy studies.

References

[1] J.E. Gray, B. Luan, J. Alloys Compd. 336 (2002) 88.
[2] E.W. Pluddenum, in: A.A. Tracton (Ed.), Coatings Technology Handbook, Taylor and Francis Group, Boca Raton, 2006, p. 70.
[3] G. Pan, D.W. Schaefer, J. Ilavsky, Thin Solid Films 503 (2006) 259.
[4] F.D. Osterholtz, E.R. Pohl, J. Adhes. Sci. Technol. 6 (1992) 127.
[5] P. Eaton, P. Holmes, J. Yarwood, J. Appl. Polym. Sci. 82 (2001) 2016.
[6] A. Franquet, H. Terryn, J. Vereecken, Appl. Surf. Sci. 211 (2003) 250.
[7] U. Bexell, G. Mikael, O. Mikael Olsson, G. Ulrik, Surf. Interface Anal. 36 (2004) 624.
[8] A.M. Cabral, R.G. Duarte, M.F. Montemor, M.G.S. Ferreira, Prog. Org. Coat. 54 (2005) 322.
[9] P.E. Hinze, M.C. Luz, Electrochim. Acta 51 (2006) 1761.
[10] B. Tao, C. Xian-Hua, Wear 261 (2006) 730.
[11] F. Zucchi, V. Grassi, A. Frigani, C. Monticelli, G. Trabanelli, Surf. Coat. Technol. 200 (2006) 4136.
[12] J. Kim, K.C. Wong, P.C. Wong, S.A. Kulinich, J.B. Metson, K.A.R. Mitchell, Appl. Surf. Sci. 253 (2007) 4197.
[13] A.N. Khramov, V.N. Balbyshev, L.S. Kasten, R.A. Mantz, Thin Solid Films 514 (2006) 174.
[14] Z.-C. Liu, Q.-G. He, P. Hou, P.F. Xiao, N.Y. He, Z.H. Lu, Colloids Surf., A 257 (2005) 283.
[15] E. Finocchio, E. Macis, R. Raiteri, G. Busca, Langmuir 23 (2007) 2505.
[16] G. Song, A. Atens, M. Dangusch, Corros. Sci. 41 (1999) 249.
[17] E.F. de Oliveira, Y. Hase, Vib. Spectrosc. 25 (2001) 53.
[18] S. Ardizzone, C.L. Bianchi, M. Fadoni, B. Vercelli, Appl. Surf. Sci. 119 (1997) 253.
[19] C.F. McConville, D.L. Seymour, D.R. Woodruff, Surf. Sci. 1 (1988) 188.
[20] J.A. Taylor, J. Vac. Sci. Technol. 20 (1982) 751.
[21] T.J. Horr, P.S. Arora, Colloids Surf., A 126 (1997) 113.
[22] M. Dhandapani, L. Thyagu, P. Arun Prakash, G. Amirthaiganesan, M.A. Kandhaswamy, V. Srinivasan, Cryst. Res. Technol. 41 (2006) 328.